CDF/3582/TOP/ANAL/CDFR

The SLT tags and backgrounds for 110 pb^{-1}.

May 21, 1996

C. Campagnari, D. Kestenbaum

The bulk of this note describes the results of applying the SLT tagger to the 90.3 pb^{-1} Run 1b sample. We discuss the background calculations in full detail - the derivation of the fake rate, the testing of the fake rate on various samples, the $b\bar{b}$, Drell-Yan, Z$\rightarrow$ $\tau^+\tau^-$, Wc and Z$\rightarrow$ $\tau^+\tau^-$ backgrounds. We assume a reader with infinite attention span. As a bonus we also present a Method II calcuation of the background for Run 1b. At the end we combine the results with the Run 1a numbers.

This note is almost entirely excerpted from [1]. The SLT algorithm is reviewed in CDF-3682 which is intended as a compainion to this note.

1 SLT tags in the Run 1b W+jets sample

Before discussing the backgrounds we summarize the number of SLT tags in the W+jets sample from Run 1b. (The results from Run 1a will be added at the end of the note). We apply the SLT tagger and make some additional *event* cuts to remove obvious backgrounds which are discussed next. The cuts are contained in C$TOP:SLT_TOP_CUTS.CDF (offline DEVELOPMENT) for those who wish to reproduce the results. The W+jets sample used is the standard top group sample made by Rob Roser and others.

1.1 Background Removal

The W + jets sample contains some background from non-W sources which can generate a soft lepton tag. Examples are Drell-Yan, $b\bar{b}$, J/ψ or Υ production of leptons. Fortunately many of these events can be removed with simple cuts which do not significantly reduce the top acceptance.

1.1.1 Drell-Yan

The Drell-Yan process ($p\overline{p} \rightarrow l^+l^-X$) can produce a lepton which passes the primary cuts, and a second which is soft lepton tagged. Although there are generally no neutrinos associated with Drell-Yan production, mismeasured jet energies can result in $\not{E}_t$ and place the event in the W sample. For Drell-Yan pairs, the primary lepton and the SLT will have the same flavor and opposite charges, and will typically be isolated. Isolation for a soft electron is defined as

$$Iso^{(soft\ e)} = \frac{E_t^{cone} - E_t^{ele}}{E_t^{ele}}$$

	W + 1 jet	W + 2 jets	W+3 jets	W + $\geq$ 4 jets
Drell-Yan removal	49	15	1	0
Drell-Yan (same charge)	10	2	1	0
Low Mass removal	10	1	0	1
Upsilon removal	5	0	1	0
Residual Z$\rightarrow \mu^+\mu^-$ removal	4	5	0	0

Table 1: The number of events identified by the various background removal cuts. Since there is some overlap, the numbers given for each are after the removal algorithms above have already been applied.

where E_t is the transverse (electromagnetic) energy of the soft electron, and E_t^{cone} is the transverse energy (hadronic and electromagnetic) in a cone of $R = 0.4$ around the electron. For muons isolation is similarly defined as

$$Iso^{(soft\ \mu)} = \frac{E_t^{cone} - E_t^{tower}}{P_t}$$

where E_t^{tower} is the energy in the calorimeter tower behind the muon, and P_t is the momentum of the muon track. For the purposes of Drell-Yan removal, soft leptons with P_t >20 GeV/c are considered isolated if they have Isolation< 0.1. If the soft lepton has P_t <20 GeV/c, the requirement is loosened to $E_t^{cone} - E_t^{ele}$ <2 GeV (for electrons) or $E_t^{cone} - E_t^{tower}$ <2 GeV for muons which is equivalent to the isolation cut at P_t=20 GeV/c. Events where the primary lepton and the SLT are the same flavor, have opposite charge and are isolated are defined as Drell-Yan candidates and removed. For Drell-Yan pairs, the SLT leg is expected to have large P_t since the other has been selected as a primary lepton and so has $P_t > 20$ GeV.

To estimate the efficiency of this procedure for removing Drell-Yan pairs, a study is performed using $Z \rightarrow l^+l^-$ pairs where one lepton passes the primary cuts, and the other is tagged with the SLT algorithm. The removal procedure is found to be $87 \pm 1\%$ efficient for electron pairs, and $96.4 \pm 0.3\%$ of muon pairs. Although in these samples, both legs are higher P_t than the continuum Drell-Yan events which will appear in the W sample, the cuts are expected to be at least this efficient when the second lepton is softer and so need only pass the loosened isolation requirement.

Table 1 lists the number of Drell-Yan candidate events removed from the W+jets sample as a function of jet multiplicity. Also listed are the number of like charge pairs which *would* be removed, were they instead of opposite charge. In Section 7 this will be used to estimate the *overefficiency* of the Drell-Yan removal.

Figure 1 shows the momentum spectrum of the SLT in the Drell-Yan events. Also shown is the momentum spectrum for like charge pairs, that would otherwise be removed. As expected, many of the candidates have an SLT with large P_t.

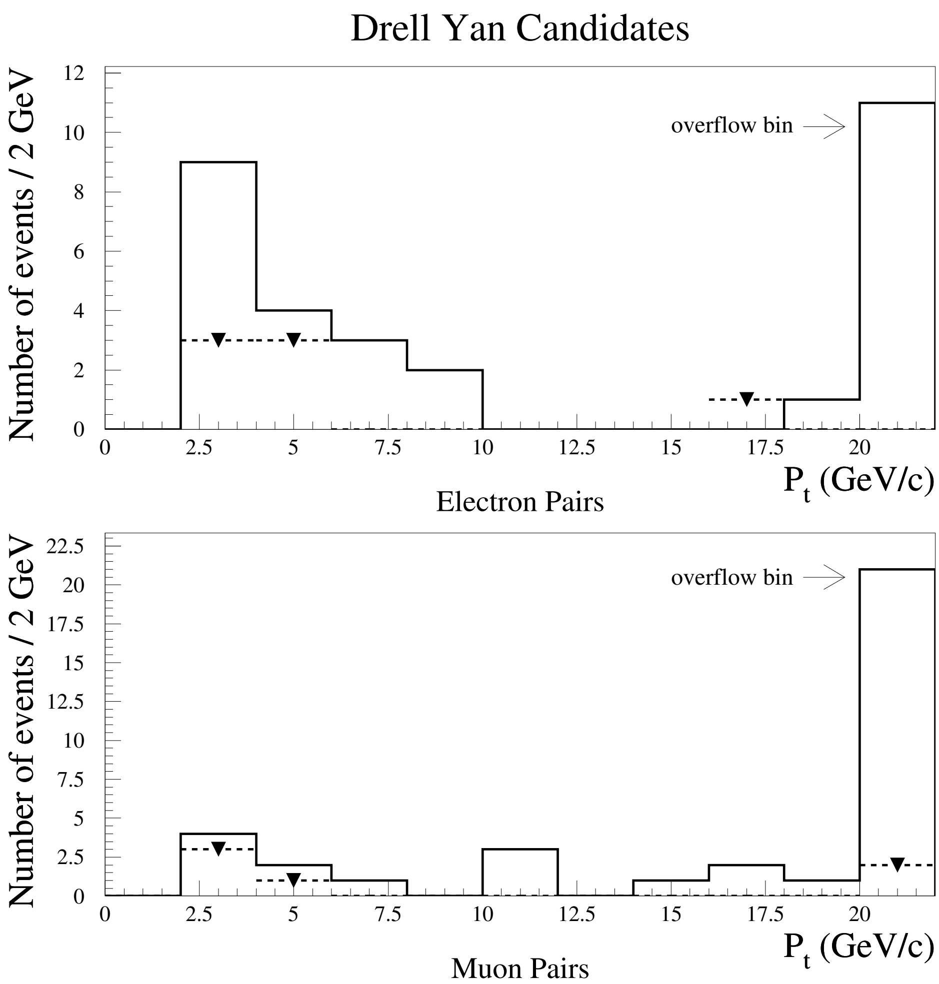

Figure 1: P_t spectrum of SLT's in events removed as Drell-Yan candidates from the W+$\geq$ 1 jet sample. The top plot shows electron events, the bottom shows muon events. In each the histogram represents the opposite charge pairs that were actually removed and the triangles represent the same charge pairs that pass all other Drell-Yan removal cuts. The highest P_t bin contains entries for $P_t \geq$20 GeV/c.

1.1.2 Low Mass Lepton Pairs

Several background processes will result in events where the invariant mass of the SLT and the primary lepton is less than 5 GeV/c^2. Lepton pairs from sequential b decay ($b \rightarrow l\nu c, c \rightarrow lX$) are expected to have low mass. Also a high P_t J/ψ or ψ' may decay to an e^+e^- or $\mu^+\mu^-$ pair where one leg appears as a primary lepton, and the other as a soft lepton. All events in which the primary and soft lepton are of opposite sign and have an invariant mass of less than 5 GeV/c^2 are removed from the sample. Figure 2 shows the mass distributions for same flavor pairs in the *inclusive* electron and muon samples (no Isolation or $\not{E}_t$ cuts applied) where the mass for opposite sign pairs has been plotted, and the same distribution for same sign pairs subtracted. The plot shows a falling distribution at low mass from sequential decays, and a mass peak for the J/ψ . In the muon plot a peak due to ψ' is also visible. Also apparent is a bump around 9.5 GeV/c^2 from the upsilon which is discussed next. There are fewer electron pairs than muon pairs because the primary electron selection criteria contain implicit isolation requirements which reduce the probability of finding a second lepton nearby.

The plot demonstrates the level of these backgrounds in the inclusive lepton samples. After the $\not{E}_t$ and isolation cuts have been applied to select the W sample, only a handful of events are removed with the low mass cuts. Table 1 lists the number of events removed as a function of jet multiplicity.

1.1.3 Upsilons

As shown in Figure 2 a mass bump corresponding to the Υ is visible around 9.5 GeV. Although the background from Υ's is expected to be extremely small in the W sample, events are removed where the primary lepton and the SLT are of opposite sign, have the same flavor and form an invariant mass 8 GeV/c^2 <M$_{primary+SLT}$ <11 GeV/c^2, since it would be hard to justify a top candidate event where the SLT and primary lepton formed an invariant mass near the Υ mass. There is, in fact, one such event removed from the W+3 jet bin. Table 1 lists the number of events removed as Υ candidates in the W sample.

1.1.4 Z Bosons (second pass)

The standard top group Z removal has already been applied to the W sample. However, since this analysis is particularly susceptible to backgrounds processes which produce two leptons, further cuts are required. In particular, since the standard Z removal makes isolation and minimum ionizing cuts on the second muon leg, it may miss a lepton if there is jet activity in the event which overlaps with the lepton, and since the SLT algorithm is designed to identify leptons in jets, it may find these. Events where the primary and SLT have opposite charge, are of the same flavor and make a mass 70 GeV/c^2 <M$_{primary+SLT}$ <110 GeV/c^2 are removed from the sample. Table 1 lists the number of events removed as $Z \rightarrow \mu^+\mu^-$ candidates.

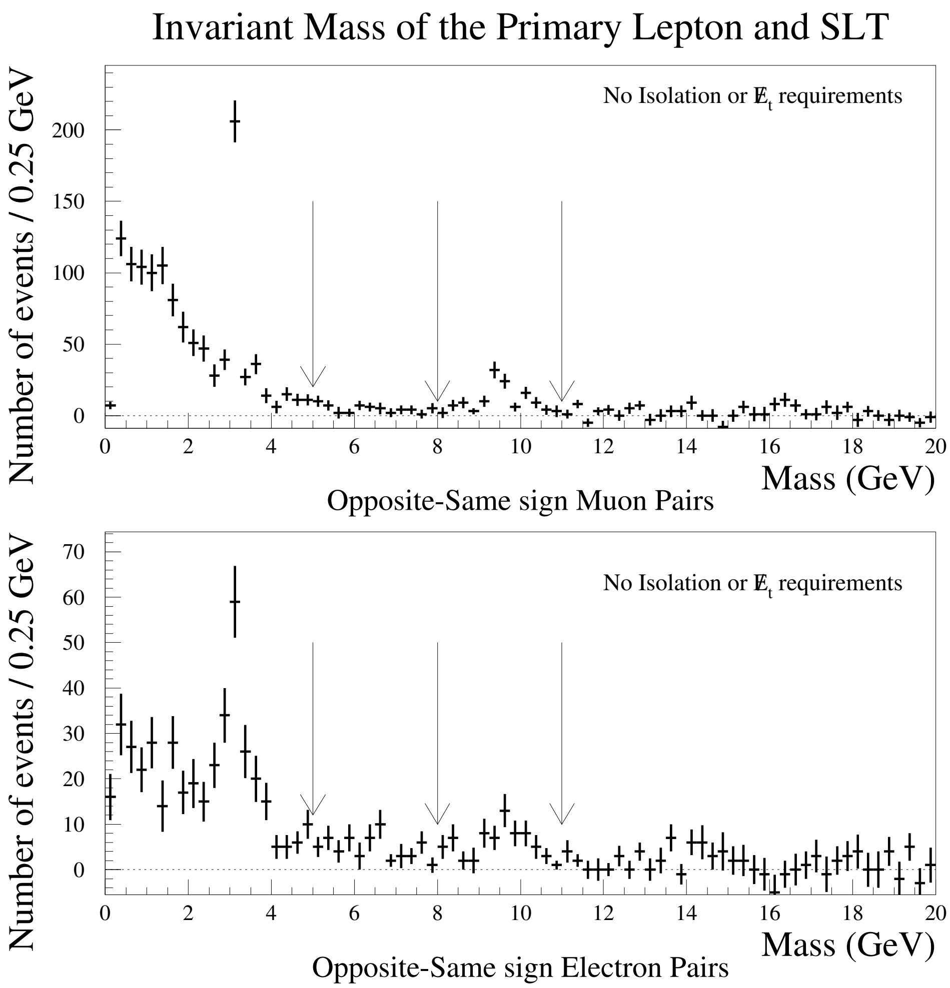

Figure 2: The invariant mass of same flavor primary lepton and SLT pairs in the inclusive lepton sample. Shown is the mass for opposite sign leptons with the distribution for same sign pairs subtracted. Drell-Yan pairs have been removed as described above. Visible are the low mass hump from the sequential decay $b \rightarrow l\nu c, c \rightarrow lX$, and mass peaks from the J/ψ, ψ' (for muons) and the Υ. Events with primary-SLT pair masses below 5 GeV/c^2 or between 9 and 11 GeV/c^2 are removed. Note also that there is no excess of events for larger masses. After the Isolation and $\not{E}_t$ requirements have been imposed to select the W sample, only a handful of events are removed by these cuts. (See Table 1.)

Jet multiplicity	Events	Soft lepton tags	Soft lepton tagged events	Double tags
W+1 jet	9001	201	197	4
W+2 jets	1376	66	66	0
W+3 jets	212	23	21	2
W+ $\geq$ 4 jets	61	15	13	2

Table 2: The number of events before tagging, the number of soft lepton tags, and the number of soft lepton tagged events in the Run 1b W+jets data sample. There are four double tagged events in the W+$\geq$3 jet bin and four in the W+1 jet bin.

2 Soft Leptons in the W+Jets Sample

Figure 3 shows the number of soft lepton tags found in the W+jets sample as a function of jet multiplicity. The background removal cuts described above have already been applied. Table 2 lists the number of events, tags and tagged events as a function of jet multiplicity. There are four double tagged (two soft lepton tags) events in the W+1 jet bin, none in the W+2 jet bin, two in the W+3 jet bin and two in the W+$\geq$4 jet bin. Requiring a soft lepton tag has reduced the number of events in the W+$\geq$3 jet bin by a factor of seven.

3 The SLT Backgrounds

The major background to the top signal in this analysis comes from "fake" soft lepton tags. Fake tags can be defined as particles identified as leptons whose origin is not a heavy flavor decay. This includes non-leptons which pass the lepton selection cuts (such as a pion faking an electron or a muon) as well as electrons from conversions or muons from pions or kaons which decay in flight. Other backgrounds can come from W bosons produced with real heavy flavor pairs (W$b\bar{b}$, W$c\bar{c}$). Backgrounds from these three processes (fakes, W$b\bar{b}$ and W$c\bar{c}$)are estimated à la Method I with a track based fake rate derived from a sample of "generic jets" which are not expected to be enhanced in heavy flavor.

There are other background processes that can produce a W and a SLT that are not accounted for by the fake rate. These include the production of a W with an associated charm quark (Wc) and diboson (WW,WZ,ZZ) production.

Non-W backgrounds can persist in the sample and contribute real soft lepton tags that have not yet been accounted for. These include backgrounds from $b\bar{b}$, Z$\rightarrow$ $\tau^+\tau^-$ production, and residual Drell-Yan events not removed by the event cuts

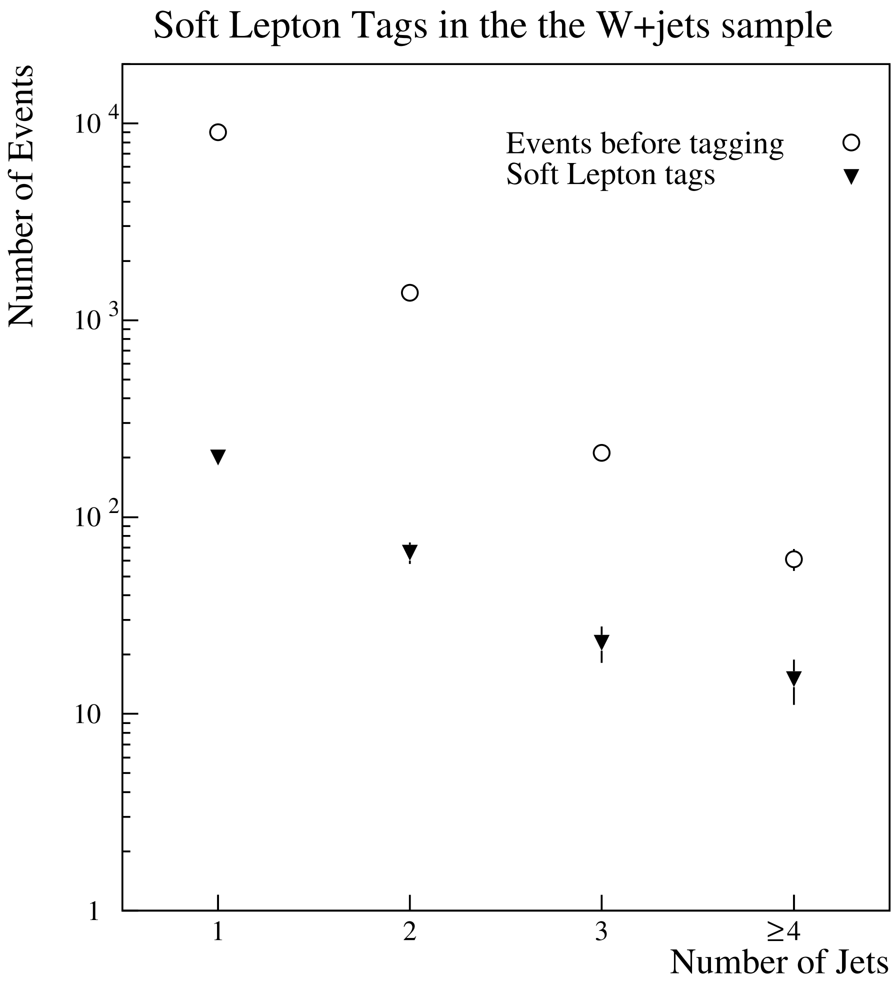

Figure 3: Shown are the number of W+jets events before and after the application of the soft lepton tagger. The last multiplicity bin is an overflow bin corresponding to events with at least four jets. The data is for Run 1b only. Results from Run 1a are added in Section 17.

(Section 1.1).

4 The Soft Lepton Fake Rate from Jet Data

4.1 Definition of the Fake Rate

The fake rate is defined as the fraction of candidate tracks[1] which pass the soft lepton id cuts described in CDF-3682. Since the fiducial regions for CMU-only, CMP-only and CMUP muons all overlap, a combined "CMU/P" muon fake rate is used which includes all these types and is defined as the number of SLT CMU-only muons, CMP-only muons and CMUP muons divided by the number of tracks extrapolating to the combined CMU and CMP regions (Types 1, 2, or 3 as defined in CDF-3682). The CMX fake rate is defined as the number of good CMX muons divided by the number of tracks that extrapolate to within the CMX boundary. For soft electrons the fake rate is defined as the number of good electrons divided by the number of fiducial electron tracks (see CDF-3682). Unless otherwise stated, the fake rates are obtained from a combination of Jet 20, 50, and 70 triggers. In these samples, 75 % of candidate lepton tracks are within a cone of 0.4 of a jet with $E_t > 15$ GeV.

4.2 Determination of the Muon Fake Rate

Since the muon matching cuts are dependent on P_t, and since the background may have a P_t dependence, the muon fake rate is parameterized as a function of the track P_t.

There is a trigger bias to the fake rate which can be seen by plotting the fake rate for all tracks in the event, and for tracks which are well separated from a trigger jet. As shown in Figure 4, the rate for tracks which are well separated from a trigger jet have a fake rate which is $\sim$ 15 % larger than the rate for all tracks. This can be understood as a consequence of the trigger requirement that the jet be over a particular threshold; jets which contain a muon (from decay in flight for instance) will have their energy measured systematically low in the calorimeter, and are hence less likely to pass the trigger. Because the underlying jet E_t distribution is steeply falling, lost energy from muons can have a large effect. By the same argument, non-trigger jets are *more* likely to have a muon since they by definition have less energy than the trigger jet. The bias, however, is entirely removed when the fake rate is calculated from tracks which are well separated from a trigger jet ($\Delta R > 0.7$). This means that if both jets fire the trigger, all tracks in the event are used. Figure 4 also shows the unbiased rate divided by the biased rate. As expected, the size of the effect increases with P_t where the energy carried away by the muon is larger.

Figure 5 shows the (unbiased) muon fake rates as a function of P_t obtained from $\sim$ 3 million tracks. To test for a possible isolation dependence, the fake rate is plotted as a function of $\Sigma_p^{0.2}$ after correcting for the P_t dependence in Figure 6.

[1] Candidate tracks are those tracks which are fiducial and have $P_t > 2$ GeV/c. See CDF-3682 for details.

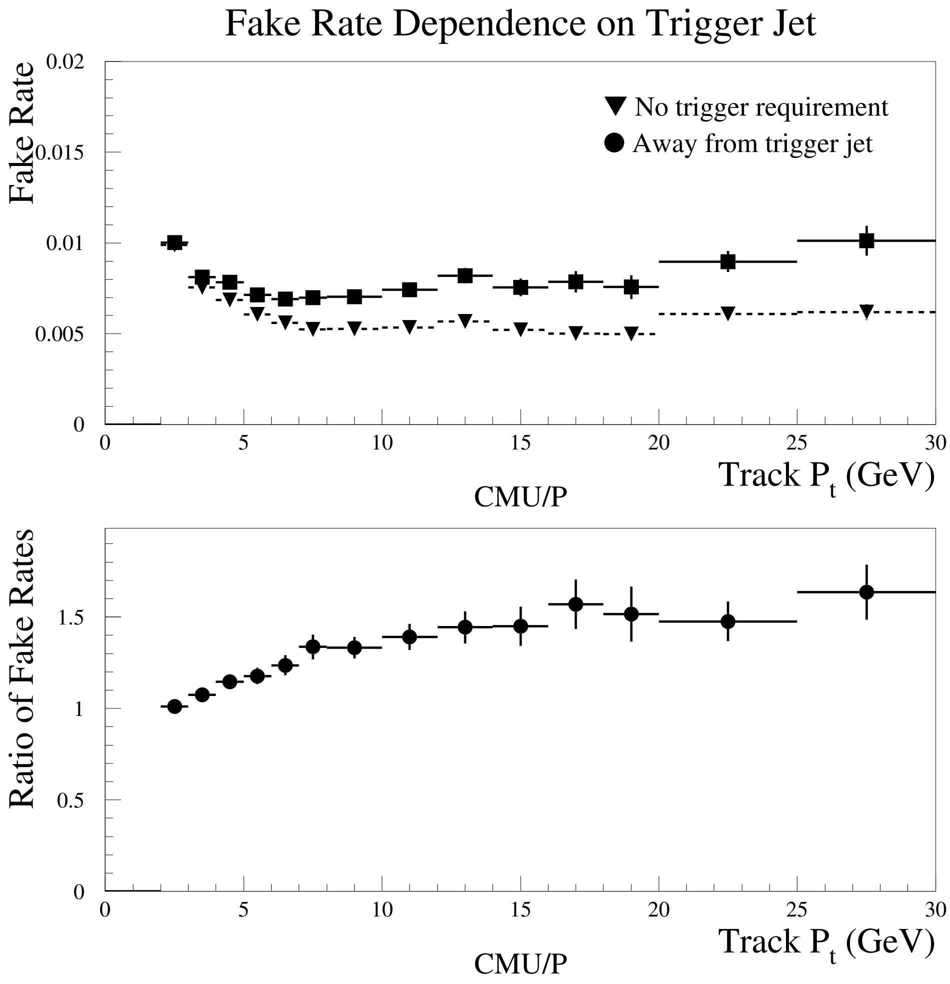

Figure 4: Top plot: CMU/P fake rate as a function of track P_t in jet events shown for all tracks (circles) and for tracks which were required to be away from a jet which passed the trigger (triangles). Bottom plot: The ratio of the fake rate for tracks away from trigger jets to the fake rate for all tracks. Jets containing muons are less likely to fire the trigger since they will have their energy measured systematically low. The rate for tracks well separated from a jet which would have caused the trigger to fire, is free from trigger bias. The effect is more pronounced at high P_t where the energy carried away by the muon is greater.

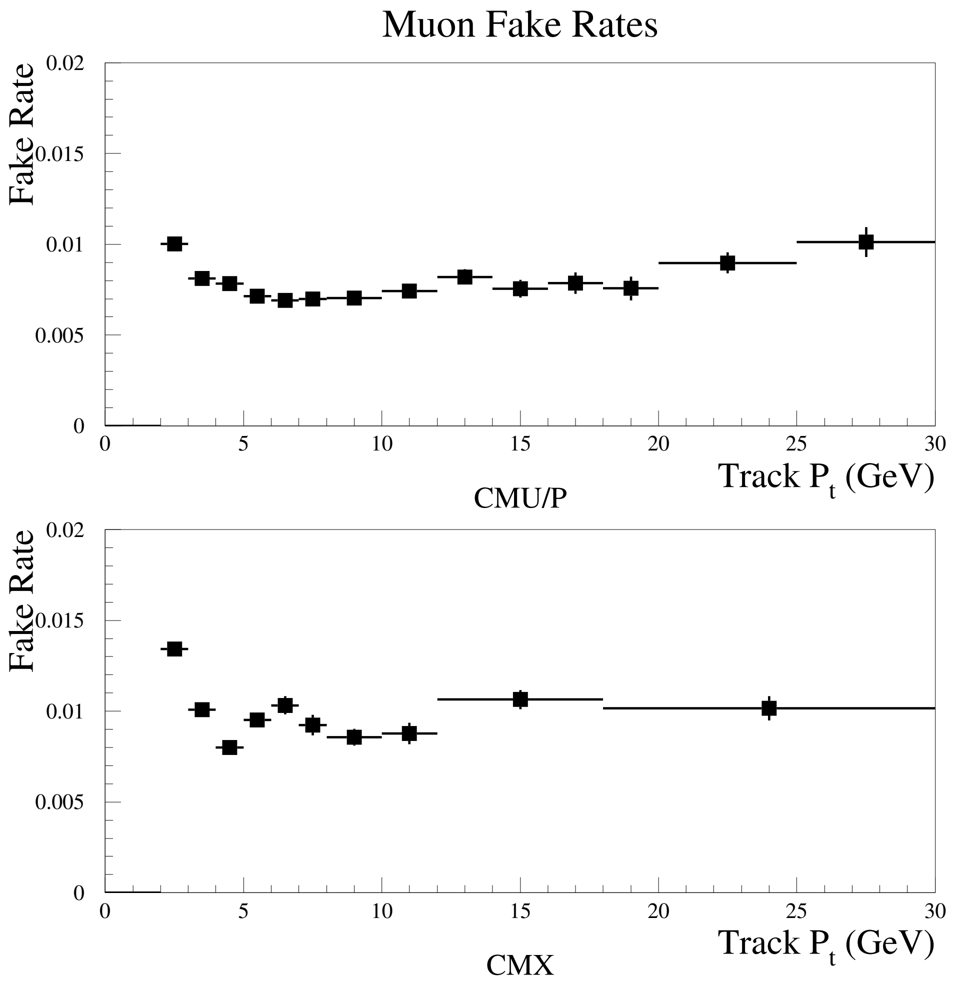

Figure 5: The fake rate for tracks extrapolating to the CMU or CMP (top) and to the CMX (bottom). The fake rate initially drops with P_t in part because the cut on matching chi-square becomes tighter with increasing P_t where multiple scattering is reduced for real muons. The selection criteria for the CMX change at P_t=5 GeV/c (Section) which causes a kink in the fake rate.

Within statistical uncertainties no correlation is observed. The fake rate is around 1 % for tracks with $P_t = 2$ GeV/c and falls for higher P_t. This behavior is in part a consequence of the matching chi-square requirements which effectively apply a tighter matching cut for higher P_t tracks.

4.3 Determination of the Electron Fake Rate

The soft electron fake rate is expected to be dependent on both isolation and track P_t. The isolation of a track can be characterized by a quantity $\Sigma_p^{0.2}/P$where $\Sigma_p^{0.2}$ is is the sum of track momentum in a cone of R=0.2 around the track, and P is the track momentum. Figure 6 shows the electron fake rate as a function of $\Sigma_p^{0.2}/P$. The final fake rate is broken up into three bins, $\Sigma_p^{0.2}/P< 0.2$, $0.2 < \Sigma_p^{0.2}/P< 5.$, and $\Sigma_p^{0.2}/P> 5$. $\Sigma_p^{0.2}/P$has been chosen instead of just $\Sigma_p^{0.2}$ because isolation dependent

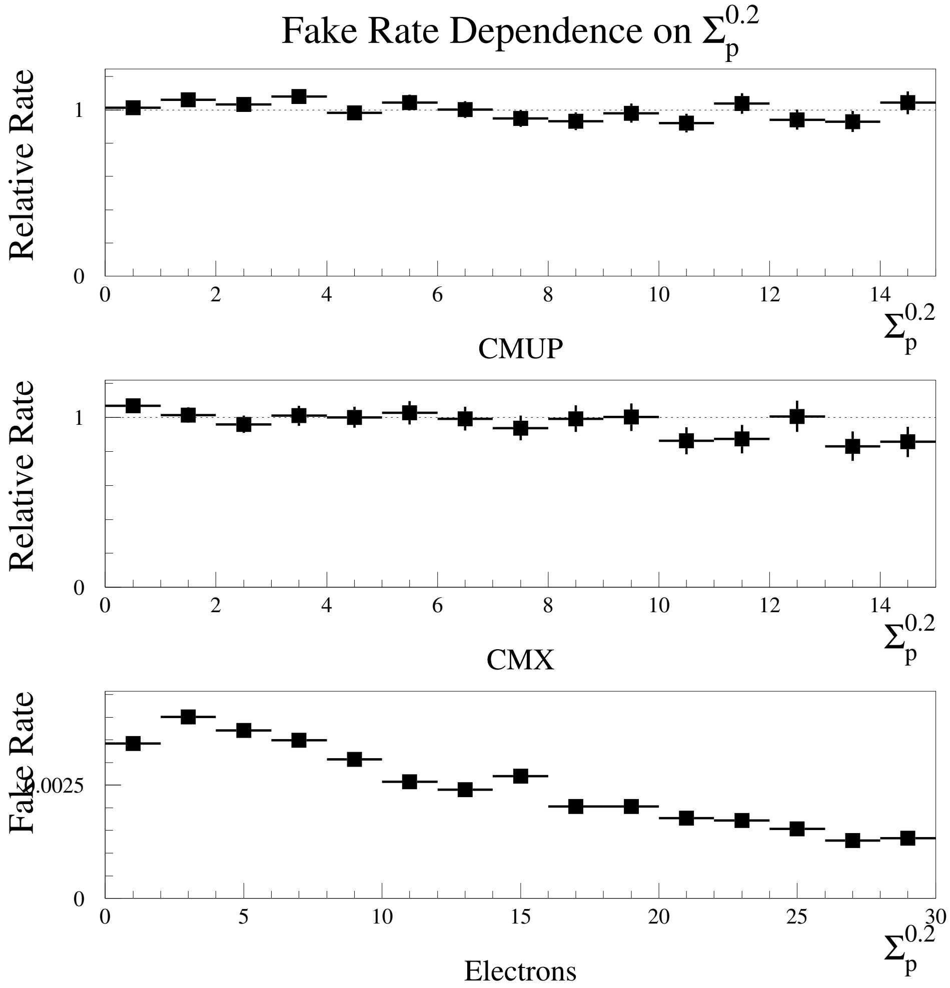

Figure 6: The muon fake rates as a function of $\Sigma_p^{0.2}$ for tracks extrapolating to the CMU/P (top) and CMX (middle) regions where the momentum dependence shown in Figure 5 has been removed. Also shown (bottom) is the electron fake rate as a function of $\Sigma_p^{0.2}$. Because of this dependence, the electron fake rate is calculated in three bins of $\Sigma_p^{0.2}$ /P.

cuts (E_{had}/E_{em} and E/p) effectively divide by the track momentum. The final rates obtained from $\sim$ 4 million tracks are shown in Figure 7. The fake rate is lowest in the $\Sigma_p^{0.2}/P>$ 5 bin because the track is less likely to pass the E_{had}/E_{em} and E/p cuts.

5 Systematic Uncertainty on the Fake Rate

The uncertainty of the Fake Rate can be determined by applying it to a variety of samples and comparing its predictions with the observed number of tags. This covers uncertainties due to the parameterization and variations in the heavy flavor content of the samples.

5.1 Check of Fake Rate Using Jet Samples

The simplest way to assess the reliability of the fake rate is to compare it across jet samples. A fake rate, for instance, can be calculated with the JET20 sample, and then applied to the combined JET50 and JET70 samples. Table 3 shows the predicted and observed tags using fake rates calculated using a single jet sample, and applying it to the remaining two. The uncertainties listed are statistical from the fake rate itself.

The fake rate performs least well for soft electrons. In the case where the rate was derived from the JET20 sample and applied to the combined JET50 and JET70 samples, 27 % more tags are predicted than observed. The rate derived in the JET70 sample, applied to the combined JET20 and JET50 sample underestimates the number of tags by 9%. It might seem that given the variation in fake rates between the three isolation bins, the situation could be improved by better accounting for the isolation dependence. A few alternative techniques have been investigated which include finer $\Sigma_p^{0.2}/P$binning, smoothing the entire distribution in the $\Sigma_p^{0.2}/P$vs P_t plane to obtain a continuous fake rate, and applying a straight line extrapolation between the three bins to estimate the fake rate for intermediate values of $\Sigma_p^{0.2}/P$. In each case no significant improvement in the ability of the electron fake rate to predict the number of tags in other samples was observed. Since the fake rate drops for higher Jet E_t triggers, it seems likely that there remains an isolation dependence which is not characterized by $\Sigma_p^{0.2}/P$. Since the accuracy of this method of calculating the background is eventually limited by the uncertainties on the heavy flavor content of generic jets compared to the W sample, and since electrons comprise less than a third of the SLT acceptance, this is not pursued further. The agreement betwen the muon predictions and the observed tags is excellent, and is at the level of the statistical uncertainty expected from the fake rate.

5.2 Check of Fake Rate Using the Photon Sample

While the test of the fake rate using the generic jet samples says something about its predictive power in a sample selected in a similar manner to the one it was derived from, it should also be tested on completely unrelated events. In particular it is useful to look in samples where the heavy flavor content is expected to be different from the

Electron fake rate

Fake Rate from	Test Sample	Predicted	Observed	Difference/Observed
JET 20	JET50+JET70	8814 ± 201	6939	+ 27 %
JET 50	JET20+JET70	6596 ± 114	6790	- 3 %
JET 70	JET20+JET50	5912 ± 101	6459	- 9 %

Muon fake rate

CMU/P				
Fake Rate from	Test Sample	Predicted	Observed	Difference/Observed
JET 20	JET50+JET70	12019 ± 219	11782	- 2 %
JET 50	JET20+JET70	10128 ± 138	10015	-1 %
JET 70	JET20+JET50	8886 ± 112	8939	-0.6 %
CMX				
JET 20	JET50+JET70	6091 ± 147	6283	- 3 %
JET 50	JET20+JET70	5459 ± 101	5428	+ 1 %
JET 70	JET20+JET50	5004 ± 87	4879	+3 %

Table 3: The predicted and observed tags for fake rates obtained from generic jet samples collected with different triggers. In each case the fake rate is applied to an independent sample. For example the fake rate derived from the JET20 sample is applied to the combined JET50 and JET70 samples. The muon fake rate predictions agree with the observed tags to a few percent which is within the statistical uncertainty expected, the electron fake rate performs less well across samples.

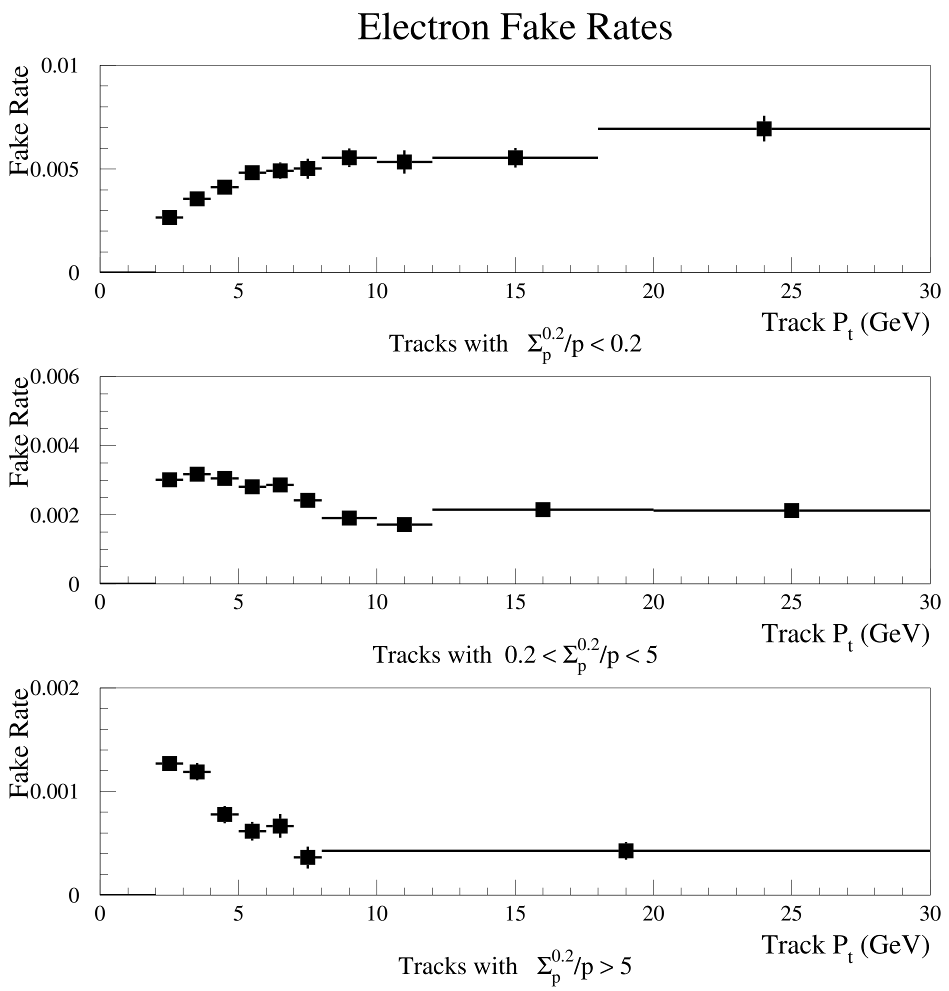

Figure 7: The electron fake rate as a function of track P_t for three different bins in $\Sigma_p^{0.2}$ /P. The fake rate drops with increasing $\Sigma_p^{0.2}$ /P where tracks are less likely to pass the E/p and E_{had}/E_{em} cuts.

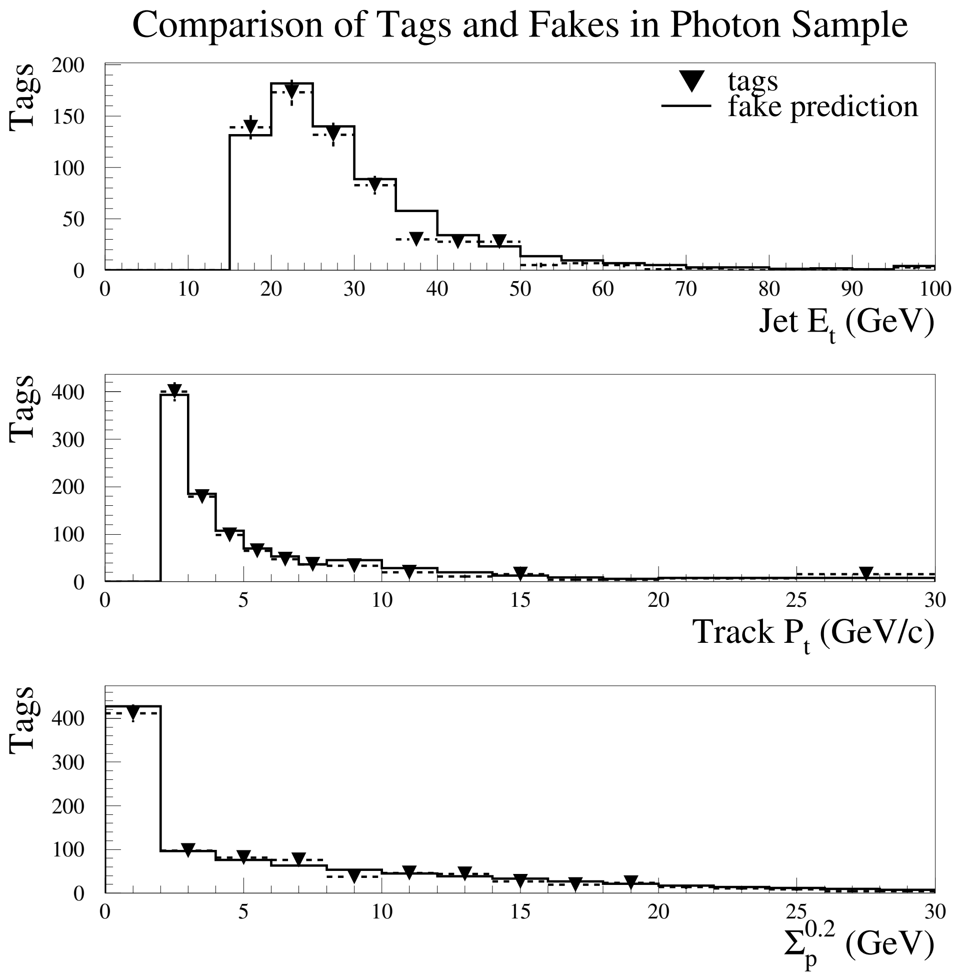

Figure 8: In the photon sample, the track P_t, $\Sigma_p^{0.2}$ and E_t of jet in a cone of ΔR=0.4 around the soft lepton (triangles) and as predicted by the fake rate (histogram).

generic jet sample. To this end, the fake rate is applied to a "photon plus jet" sample from the CEM_23 triggers. Offline photons are selected by requiring that no 3-D tracks extrapolate to the cluster. The final sample selection requires an additional jet with at least 15 GeV of transverse energy and contains 44053 events. This sample was prepared by Weiming Yao.

In the photon+jet sample, additional heavy flavor is expected from charm quarks in the proton sea which scatter off a gluon and produced a photon. Table 4 compares the predictions from the fake rate with the found tags. The agreement for the CMU/P muons and for the electrons are both within the expected statistical uncertainty from the number of found tags. The prediction for CMX muons is 16 % high, although there is an 8% statistical uncertainty from the number of observed tags. Combining all SLT types, 985 tags are predicted and 935 observed. Overall the prediction is high by 5%.

It is useful to compare also the distributions for the tags to the predictions from fake rates. In Figure 8 the expected P_t, $\Sigma_p^{0.2}$ and Jet E_t distributions from the fake

SLT type	*fake prediction*	*observed tags*	Difference/Observed
CMU/P muons	498.9	478	+ 4 $\pm$ 5 %
CMX muons	246.4	211	+ 16 $\pm$ 8 %
Electrons	239.4	246	- 3 $\pm$ 6 %
TOTAL	984.7	935	+5 $\pm$ 3 %

Table 4: Test of the fake rate in the photon + jet sample comparing the expected tags calculated using the fake rate to the number of observed tags.

rates is compared to the distributions for the actual tags. Here Jet E_t refers to the jet within a cone of ΔR=0.4 of the SLT. (If the SLT is not near a jet, it does not appear in this plot.) For all three variables the agreement is good, indicating that the fake rates have been parameterized in a sensible manner, and that there are no unexpected biases such as an excess of tags in high energy jets.

5.3 Check of Fake Rate Using the Z Sample.

The Z sample (again standard top group selection) provides a good check of the fake rate while also testing the validity of the assumption that it can be applied to the W sample. If there were an anomalous source of heavy flavor in W events (not due to top) this might also be apparent in the Z sample. In this sense the Z's provide the perfect control sample - a selection of high-purity vector bosons with no expected top component.

Unfortunately there are an order of magnitude fewer Z's than W's produced which decay to charged leptons, and so statistics are limited. The predicted and observed tags as a function of jet multiplicity are listed in Table 5. Within the limited statistics available, the agreement is excellent. Overall 83 tags are expected and 82 observed.

5.4 Systematic Uncertainty of the Fake Rate

Based on the above three studies a 20% uncertainty is assigned to the electron fake rate and a 10% uncertainty to the muon fake rate. Since these uncertainties are expected to be largely uncorrelated, the systematics are added in quadrature when predictions from the two are combined. The statistical error on the fake rate is ignored since this is much smaller in all cases ($\sim$ 3%).

6 Application of the Fake Rate to the W Sample

The fake rate applied to the W sample predicts 202 $\pm$ 18 tags in the W+1 jet bin, 57 $\pm$ 5 tags in the W+2 jet bin, 13.2 $\pm$ 1.2 in the W+3 jet bin and 6.1 $\pm$ 0.6 in the

	Z+0 jets	Z+1	Z+2	Z+≥3	Z+any
Number of events	8586	861	129	18	9594
CMU/P fake prediction	24.9	11.2	3.0	0.7	39.8
CMU/P tags observed	24	9	1	1	36
CMX fake prediction	16.1	5.4	1.6	0.2	23.3
CMX tags observed	19	6	0	0	25
Electron fake prediction	12.7	5.2	1.4	0.3	19.6
Electron tags observed	15	5	1	1	21
TOTAL predicted	53.7	21.8	6	1.2	82.8
TOTAL observed	58	20	2	2	82

Table 5: Expected tags calculated using the fake rate and observed tags in the Z sample. Overall 83 tags are predicted by the fake rate and 82 are observed.

W+≥4 jet bin. The results are summarized in Table 10.

7 Drell-Yan background

7.1 Drell-Yan Removal Underefficiency

Although Drell-Yan candidates where both legs are isolated have already been removed (Section 1.1) , some may remain, especially if there is jet activity in the event which can overlap with one of the leptons. The underefficiency of the removal criteria is estimated by applying them to a sample of Z + jets events, where the Z decays to leptons, one which passes the primary lepton cuts, and the other which is tagged as an SLT. It is found that the Drell-Yan removal identifies 1598 out of 1842 $Z \rightarrow e^+e^-$ events, and 2760 out of 2857 $Z \rightarrow \mu^+\mu^-$ events. The underefficiency of the removal then, is 13 $\pm$1% for electrons and 3.4 $\pm$0.3% for muons. Figure 9 shows the isolation for electrons and muons from Z's.

The underefficiency is likely to be effected by jet activity in the event, and so is calculated separately for Z+ $\geq$ 1 jet and Z+ $\geq$ 2 jets. The results are shown in Table 6. Although the statistics are low, the removal is clearly less efficient when there are other jets in the event. The numbers in the Z+$\geq$ 2 jet bin compare well with the isolation efficiency for leptons from W's in top Monte Carlo which is on the order of 85 %.

One might worry that the P_t of leptons from Z decay will be larger than the P_t of the leptons from Drell-Yan production which may end up in the sample. The isolation variable used to identify Drell-Yan candidates in particular, could become less efficient at low P_t. However, as discussed in Section 1.1, this is not expected to be

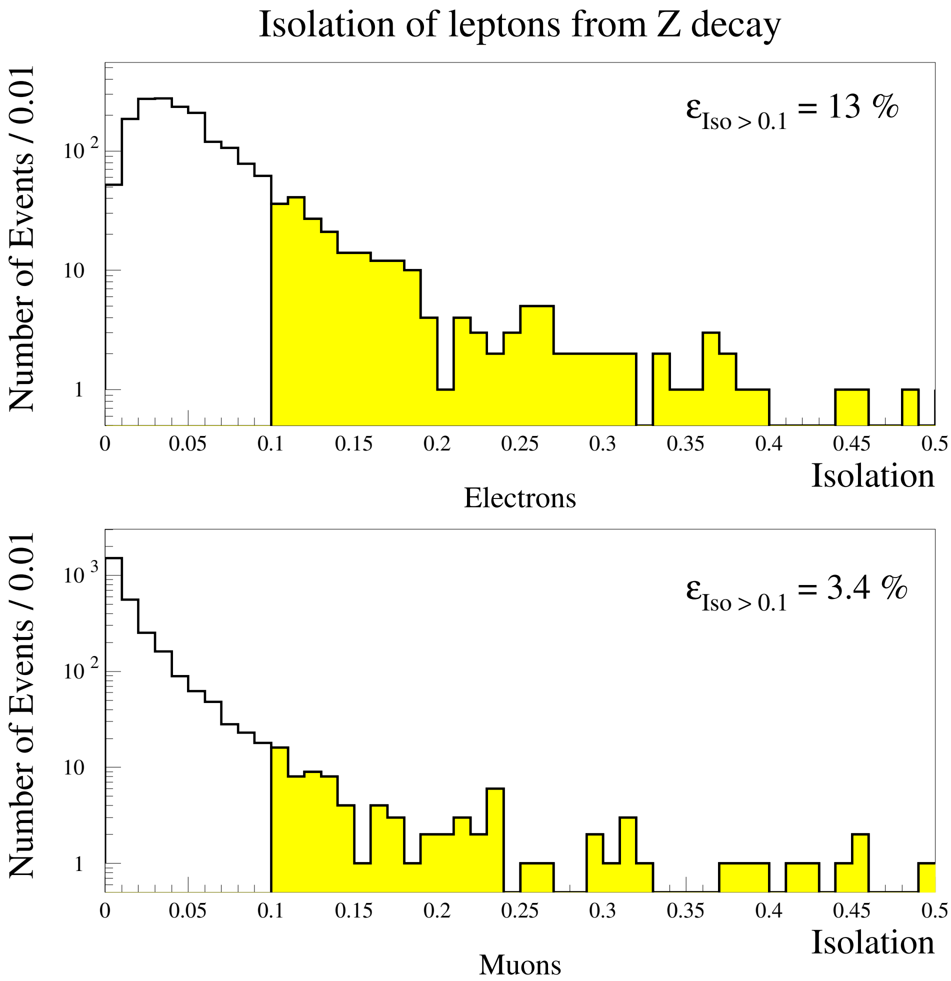

Figure 9: Isolation (I) for electrons and muons from Z decay selected with the SLT algorithm. The fraction of events with $I > 0.1$ gives the overefficency of the Drell-Yan removal. The overefficiency increases with jet multiplicity as shown in Table 6.

Jet Multiplicity	Electrons	Muons
Z+any	13.2 $\pm$ 0.8 %	3.4 $\pm$ 0.3 %
Z+$\geq$ 1 jet	18 $\pm$ 3 %	10 $\pm$ 2 %
Z+$\geq$ 2	36 $\pm$ 10 %	18 $\pm$ 6 %

Table 6: The underefficiency of the Drell-Yan removal algorithm in $Z \rightarrow l^+l^-$ events as a function of jet multiplicity.

a problem since SLT's with with $P_t < 20$ GeV/c are removed if they have $E_t^{cone} - E_t < 2$ GeV. This is less stringent than requiring Isolation<0.1 and in fact is equivalent to the isolation cut at $P_t = 20$ GeV/c. Consequently it should be an accurate estimate of the removal underefficiency.

7.2 Drell-Yan Removal Overefficiency

The loose Drell-Yan removal cuts at low P_t (see above) mean that some non Drell-Yan events will also be taken out. This must be corrected for this since these are events that are accounted for by other parts of the background estimate. If, for instance, a "fake" tag is removed as a Drell-Yan, then the estimate of the fake background will come up one event too high (if it were perfect). In a sense this is just bookkeeping.

A measure of the *overefficiency* of the Drell-Yan removal is obtained by counting the number of *same sign* pairs that pass all other Drell-Yan cuts, and would otherwise be removed. Assuming that there is no correlation between the sign of the primary and SLT in these events, the number of non-Drell-Yan's incorrectly removed should equal the number of these same-sign pairs. Table 1 lists the number of same-sign and opposite-sign pairs in the W sample.

7.3 Calculation of Remaining Drell-Yan

The number of residual Drell-Yan's is given by

$$Drell - Yan \;\; background = \frac{N_{opp.\ sign} - N_{same\ sign}}{\epsilon_{under\ efficiency}} - N_{same\ sign}$$

where $\epsilon_{under\ efficiency}$ is the underefficiency as measured from Z's, $N_{opp.\ sign}$ is the number of opposite sign pairs removed and $N_{same\ sign}$ is the number of same sign pairs that would have been removed, had they not been same sign. Subtracting $N_{same\ sign}$ compensates for the overefficiency of the removal. Where there has been more over-removal than under-removal, the resulting "background" is negative.

This calculation is performed for electrons and muons separately, with the underefficiencies from Table 6 applied as a function of jet multiplicity. For events with three or more jets with $E_t > 15$ GeV, an estimated underefficiency of 20 ± 10 % is used. The final results are listed in Table 10.

8 $b\bar{b}$ background in the W sample

Another source of non-W background in the W sample are $b\bar{b}$ events where one b decays leptonically ($b \to \ell\nu c$) producing a high P_t lepton and where neutrinos in the b decay or mismeasured jet energies result in $\not{E}_t$. These events can produce additional soft lepton tags if the decay of the other b in the event produces a lepton. Recall that events have already been removed from the W sample if the primary and the soft lepton form a low mass and consistent with the *sequential* decay of a single b (Section 1.1) so only leptons from the other b in the event are of concern.

The expected number of soft lepton tags from $b\bar{b}$ events in the W sample is calculated from two quantities.

• F_{non-W} : This is the fraction of non-W events in the W sample and is estimated by fitting a background shape to the tails of the $\not{E}_t$ and *Isolation* distributions.

• $\epsilon_{b\bar{b}}$: This is the fraction of non-W events which contain a soft lepton from the decay of a b.

Convoluting these two numbers with with observed number of W candidates in the data yields the expected number of soft lepton tags from $b\bar{b}$.

Two techniques are employed to measure $\epsilon_{b\bar{b}}$. Both methods use the low $\not{E}_t$ lepton sample which is assumed to be representative of the non-W background. The first method looks for an excess of soft lepton tags over the prediction from the fake rate, the second method identifies lepton pairs from sequential decays and uses Monte Carlo to estimate how many $b\bar{b}$ events are in the sample, and how many soft lepton tags are expected from the decay of the other b.

8.1 Hadronic Background in the W Sample

Backgrounds in the W sample can be placed in two categories. The first are diboson events or Z bosons which produce a primary lepton, either directly or through the decay of a τ, but are not removed as Z's. The second source, is *hadronic* background, where a generic jet-type event produces something which is identified as a primary lepton. This hadronic component (which shall be refered to as "non-W" for simplicity) contains leptons from b decay and so is the quantity of interest here. In general these leptons from hadronic background (which can be real or fake) are not isolated and so the non-W component of the W sample can be estimated by extrapolating a background distribution into the signal region from the low $\not{E}_t$ and the high lepton isolation (I) regions. Specifically, the $\not{E}_t$ vs I plane is divided into four regions shown in Figure 8.1. Region D is the signal region and should contain mostly W's. Under the assumption that $\not{E}_t$ and I are uncorrelated for the non-W background, the non-W component of region D is given by

$$D = \frac{A}{B} \times C$$

Note that while it may seem reasonable that $\not{E}_t$ and I are uncorrelated for a particular background (eg. light quark jets or $b\bar{b}$) in general the *sum* will have some correlation. (Consider the simple case where one distribution has $I < 0.1$ and is flat in $\not{E}_t$ added to another distribution which has $\not{E}_t < 10$ GeV and is flat in I. While there is no correlation between $\not{E}_t$ and I for the individual distributions, there are large correlations for the sum.)

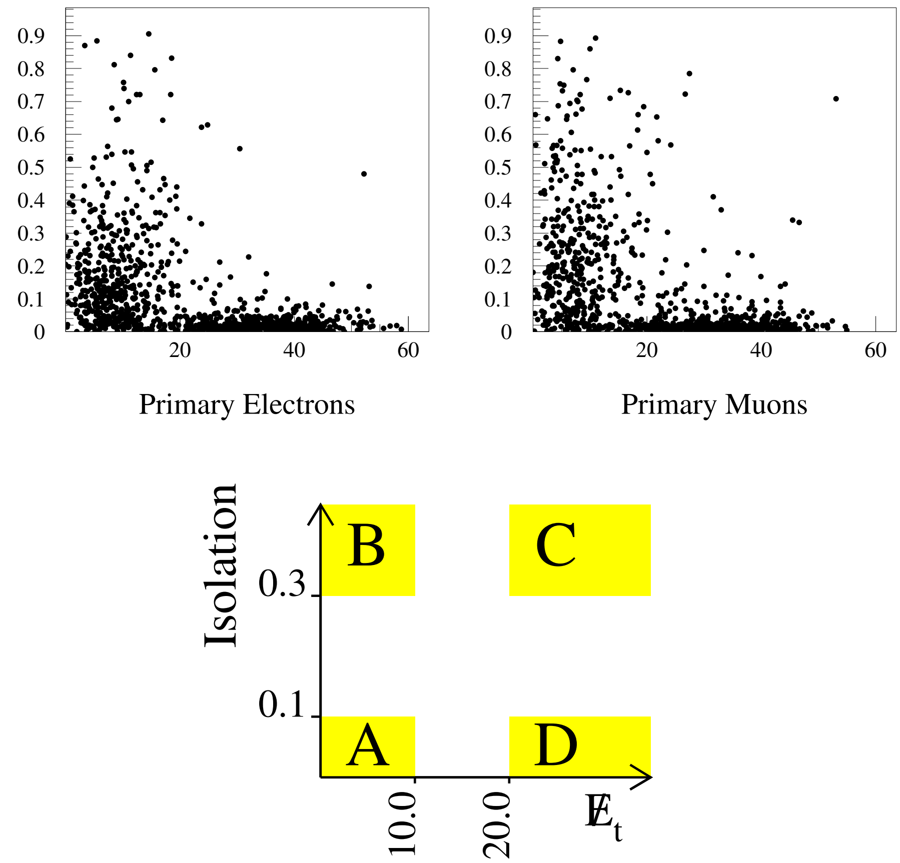

Figure 10: The regions in the $\not\!\!E_t$ - Isolation plane used to estimate the non-W component of the W sample. The A region covers $I < 0.1$ and $\not\!\!E_t < 10$, the B region covers $I > 0.3$ and $\not\!\!E_t < 10$ GeV, the C region covers $I > 0.3$ and $\not\!\!E_t > 20$ GeV. D is the signal region and corresponds to $I < 0.1$ and $\not\!\!E_t > 20$ GeV.

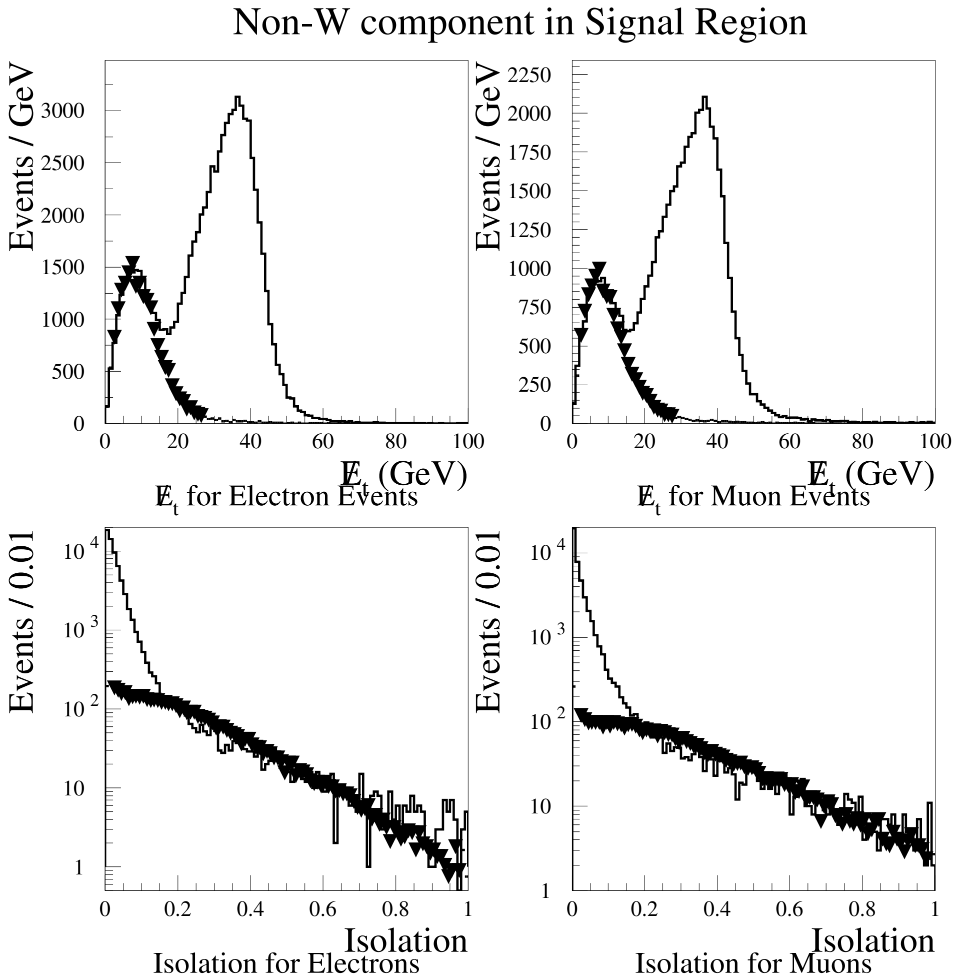

Figure 11: The $\not\!\!E_t$ distributions for inlusive leptons with Isolation (I) < 0.1 (solid) compared to leptons with $I > 0.3$ normalized to the $\not\!\!E_t < 10$ GeV region (triangles). Also shown are the (log scale) Isolation distributions for leptons with $\not\!\!E_t > 20$ GeV (solid) compared to leptons with $\not\!\!E_t < 10$ GeV normalized to the $I > 0.3$ region. The agreement of the shapes in the $\not\!\!E_t < 10$ GeV region and in the $I > 0.3$ region indicate that to a good approximation, I and $\not\!\!E_t$ are uncorrelated for the non-W background.

	Electrons	Muons
W+$\geq$ 0	2.5 $\pm$ 0.1 %	2.7 $\pm$ 0.1%
W+1	9.7 $\pm$ 0.5 %	8.7 $\pm$ 0.5%
W+2	8 $\pm$ 1 %	5.3 $\pm$ 0.5%
W+$\geq$ 3	13 $\pm$ 4 %	7 $\pm$ 2%

Table 7: The non-W fraction for various jet multiplicities using the $\not{E}_t$ vs Isolation method described in Section 8.1.

This method is essentially a poor man's fit of the $\not{E}_t$ and I distributions as seen in Figure 11 which shows the I distribution for the inclusive sample with $\not{E}_t > 20$ GeV overlapped with the distribution for events with $\not{E}_t < 10$ GeV normalized to C/B = 0.15 . Also shown is the analogous plot of $\not{E}_t$ for $I < 0.1$ and $I > 0.3$ scaled by A/B=1.49 . The quality of the fit in the $\not{E}_t < 10$ and $I < 0.3$ regions indicates that the to a good approximation, $\not{E}_t$ and *Isolation* are uncorrelated for the non-W background.

Table 7 lists the the measured non-W fraction as a function of jet multiplicity.

8.1.1 Systematic Uncertainties

In general, W's which "leak" into regions A and C, as well as un removed Z's and Drell-Yan events will limit the validity of the assumptions. Fortunately only the excess of tags due to $b\bar{b}$ are of concern here, and so this method should provide a reasonable estimate for these purposes. Other analyses have checked this method by estimating the various background components explicitly and show agreement at the 20 % level for inclusive W's [3]. To cover this, a 50% systematic uncertainty is assigned to the non-W fraction.

8.2 $b\bar{b}$ background, First Method

Having calculated the fraction of events in the W sample from non-W sources, the next step is to determine what fraction of the non-W events come from b's and how often they result in a soft lepton tag ($\epsilon_{b\bar{b}}$). As in the previous section, the low $\not{E}_t$ and high *Isolation* portions of the inclusive lepton sample are assumed to be identical to the non-W events in the W sample. The number of tags from $b\bar{b}$ in these events is calculated by looking for an excess of tags over the expectation from the fake rate.

Although it has already been implicitly assumed that the fractional $b\bar{b}$ content in non-W events is independent of $\not{E}_t$ and I, one could imagine that the fraction of non-W events from $b\bar{b}$ could be dependent on the *Isolation* of the primary lepton. Since region A has the same *Isolation* as the signal sample, it is used for the calculation. Events consistent with Drell-Yan production are removed as in Section 1.1.

Table 8 shows the number of tags found in lepton+1 jet events in region A, the number predicted by applying the fake rate, and the number expected from Drell-

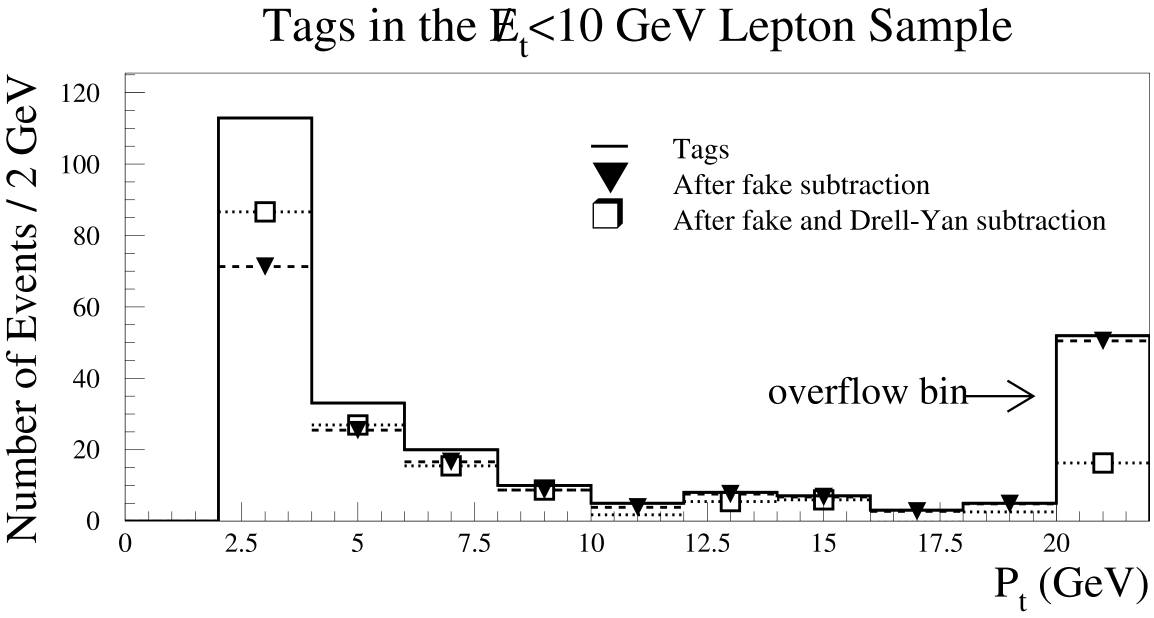

Figure 12: The P_t distribution (histogram) for soft lepton tags in events with $\not{E}_t < 10$ GeV and I <0.1 and at least one jet with $E_t > 15$ GeV. Also shown is the distribution after fakes (triangles) and the over- and under- efficiency of the Drell-Yan removal (squares) have been accounted for. The excess is assumed to come from $b\bar{b}$ events.

Yan events. Note that the Drell-Yan contribution is significant since unlike the W sample, region A has been selected my requiring $\not{E}_t$<10 GeV. Figure 12 shows the P_t distribution for soft lepton tags in region A. The number of tags with high P_t is significantly reduced after subtracting the expected Drell-Yan background, indicating that the Drell-Yan background calculation is reasonable.

Ideally these results could be broken up into the lepton+1,2,3 and $\geq$ 4 jet samples to check for a variation with jet multiplicity, but unfortunately statistics are limited and so the results from the inclusive lepton+$\geq$1 jet sample are taken to be valid for events with larger jet multiplicity. Figure 12 shows the P_t distribution of tags after backgrounds from fakes and Drell-Yan events have been subtracted. There are nearly twice as many tags as expected from fakes and Drell-Yan events. For primary electron (muon) events an excess of 97 $\pm$ 6 (73 $\pm$ 5) tags are observed in 5570 (3032) events. Thus 1.7 $\pm$ 0.2 % (24 $\pm$ 0.4 %) of the non-W events with a primary electron (muon) are expected to contain an additional soft lepton. This is the quantity $\epsilon_{b\bar{b}}$. Note that this method covers, quite generally, all possible enhancements of soft lepton tags in the non-W part of the sample, and does not explicitly assume that it is entirely due to $b\bar{b}$. The quoted errors include statistics and the systematic uncertainties on the fakes and Drell-Yan backgrounds.

Primary lepton	Number of events	Number of tags	Number of DY remaining	fake prediction	excess tag rate
Electrons	5570	169	35 $\pm$ 6	38 $\pm$ 4	1.7 $\pm$ 0.2 %
Muons	3032	87	-6 $\pm$ 3	20 $\pm$ 2	2.4 $\pm$ 0.4 %

Table 8: From inclusive leptons in the the $\not\!\!E_t < 10$ GeV, $I < 0.1$ region - the number of events, number of soft lepton tags , number of expected residual Drell-Yan events (as calculated in Section 7), the expected number of fake tags, and the final tag rate after the backgrounds have been subtracted. The uncertainties include statistics and systematics on the background subtraction. The numbers are used to calculate the excess tag rate (due to $b\bar{b}$) in the non-W part of the signal sample.

8.3 $b\bar{b}$ Background, Second Method

An alternate approach to estimating $\epsilon_{b\bar{b}}$ identifies b's directly by searching in the low $\not\!\!E_t$ sample for an SLT near the primary lepton from the sequential decay (b$\rightarrow\ell_{primary}\nu$c; c$\rightarrow\ell_{SLT}$X). A $b\bar{b}$ Monte Carlo sample where one b produces a primary lepton is then used to find the probability for finding a SLT nearby. From this, the total number of $b\bar{b}$ events in the low $\not\!\!E_t$ sample can be estimated. The same Monte Carlo sample can then be used to estimate how often the other b in these events should produce an SLT.

Sequential decays are searched for in the inclusive lepton sample with $\not\!\!E_t$<10 GeV by selecting events which have a primary electron and a soft muon or a primary muon and a soft electron. Lepton pairs from sequential decay will have opposite signs, but should be uncorrelated for other processes. Figure 13 shows the invariant mass distribution (opposite sign minus same sign) of the primary and SLT in these events. A clear excess of 197 (99) events is observed from primary-e SLT-μ (primary-μ SLT-e) pairs in the mass region below 5 GeV/c^2, where b's are expected. Same flavor pairs have not been considered because of the backgrounds from Drell-Yan and other sources, and because of the difficulty of finding a soft electron near a primary electron.

The remaining steps use a HERWIG generated $b\bar{b}$ sample. The Monte Carlo sample is selected by requiring a primary electron with E$_t$ >15 GeV. The soft lepton tagger is run on the Monte Carlo events and finds a sequential SLT-μ in 73 out of 3084 of the events, or 2.4 $\pm$ 0.3 (stat) % of the time. At the expense of statistics, the electron E$_t$ cut can be raised to E_t > 20 GeV (as is the case for the inclusive sample) which leaves 105 events containing 2.5 sequential muons[2] which gives an efficiency for finding a sequential muon of 2.4 $\pm$ 1.4(stat) %. Dividing the number of sequential decays obvserved in the data by this number should give the number of $b\bar{b}$ in the entire sample.

The final number needed is the probability to find an additional SLT from the other b in the event. Using the same $b\bar{b}$ Monte Carlo, events are selected with a

[2]In the Monte Carlo simulation, soft leptons are weighted by their tagging efficiency, so the number of tags is not an integer.

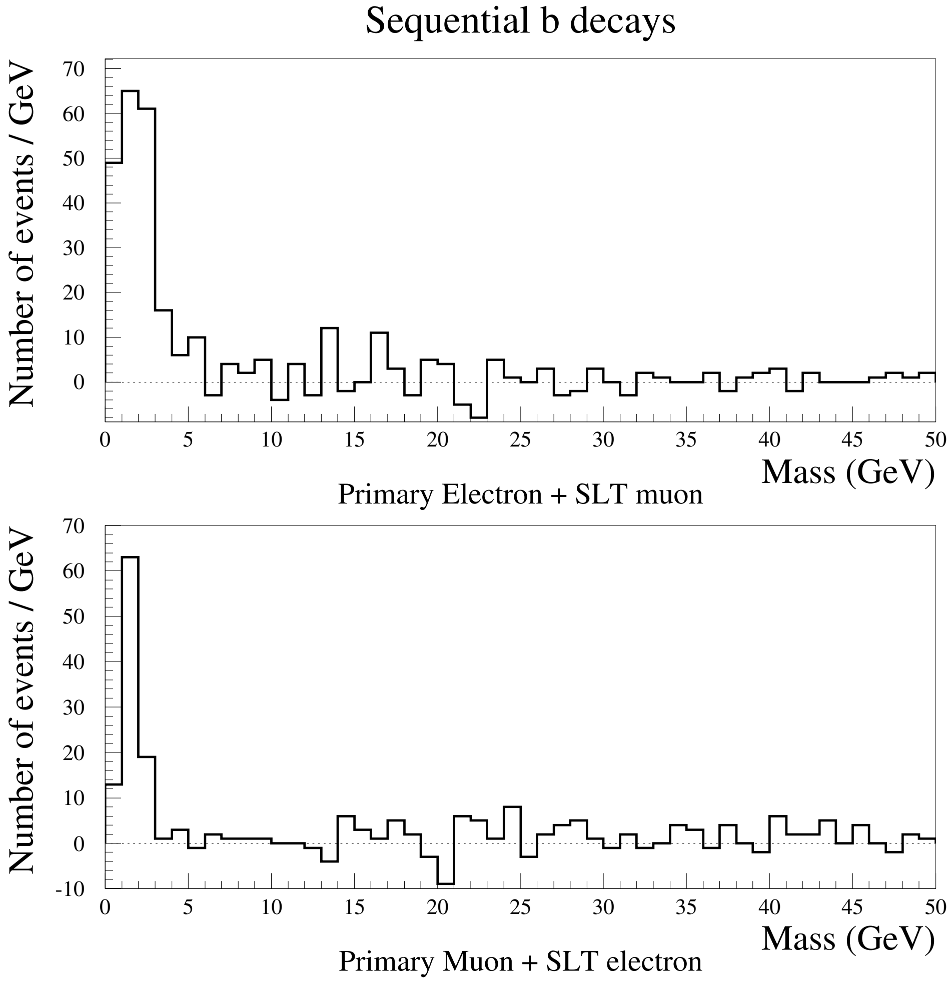

Figure 13: The invariant mass of primary and soft leptons in events with $\not{E}_t < 10$ GeV. The top histogram shows opposite sign primary-e and SLT-μ pairs with the same sign distribution subtracted. The bottom histogram shows opposite sign primary-μ and SLT-e pairs with the same sign distribution subtracted. An excess of events with mass below 5 GeV indicates the presence of b quarks decaying through $b \rightarrow l^{+(-)}c\nu, c \rightarrow l^{-(+)}\nu$.

primary electron with $E_t > 20$ GeV and a jet with $E_t > 15$ GeV. (This is similar to the region A, W+≥1 jet study above.) In 538 events, 36.5 soft leptons are found which are well separated from the primary electron, or 7 ± 1(stat) % of the time.

Turning back now to the inclusive lepton sample with $\not{E}_t < 10$ GeV, these numbers can be used to estimate the number of tags expected from the second b in $b\bar{b}$ events. First, from the sequential decay excess of 197 primary-e SLT-μ pairs and the 2.4 % efficiency for finding the sequential muon, it can be inferred that there are $\sim$ 8200 $b\bar{b}$ events in the sample. If the other b produces an additional SLT 7 % of the time, this would predict $\sim$ 574 tagged events. There are 32195 in this sample, so this corresponds to an excess fake rate of $\sim$ 1.8 %, in good agreement with the rates of 2-3 % for the first method. This also provides a rudimentary check of the Monte Carlo treatment of the soft lepton taggger.

8.4 Calculation of Residual $b\bar{b}$ Background

Because of the uncertainties associated with the $b\bar{b}$ Monte Carlo, and because the first method incorporates more generally any excess tag rate in non-W events ($c\bar{c}$ events for example), the first method is used to calculate the $b\bar{b}$ background and a conservative systematic uncertainty of 50 % assigned. The number of tags in the sample from $b\bar{b}$ production is given by

$$N^j_{b\bar{b}\ tags} = N^j_{events} \times F^j_{non-W} \times \epsilon_{b\bar{b}}$$

where $N^j_{b\bar{b}\ tags}$ is the number of W events with j jets, F^j_{non-W} is the non-W fraction for the W+j jet events, and $\epsilon_{b\bar{b}}$ is the fraction of these events expected to arise from $\bar{b}$ and produce a real soft lepton[3], taken from Table 8. The final results are listed in Table 10. The uncertainties include the 50 % systematic on the non-W fraction and the 50% systematic on the $b\bar{b}$ tag rate.

9 Wc background

Since the production of a W boson and a charm quark (through the "excitation" of a strange sea quark) is not accounted for by the fake rate, its contribution must be calculated separately. Unlike the $b\bar{b}$ background, the number of Wc events in the data cannot currently be measured and must be taken from theoretical predictions. To minimize the uncertainty on the overall Wc cross section, the *fraction* of W+jets events from Wc (F_{Wc}) is calculated from Monte Carlo. This number is then convoluted with the number of *real* W+jets events in the data, to calculate the number of Wc events in the data. To get the *real* number of W+jets events one must subtract the hadronic component calculated in 8.1 as well as the expected number of events in the sample from diboson production and unremoved Z's either where one leg was

[3]It should be noted that fake tags in non-W events have already been accounted for as part of the overall fake background since the fake rate was applied to the whole sample without subtracting the non-W component.

Jet Multiplicity	# of events	Real W fraction	F_{Wc}	$(\epsilon_{SLT\ Wc\ tag\ eff})$
W+1 jet	9001	86 $\pm$ 2 %	4.8 $\pm$ 1.3 %	2.2 $\pm$ 0.4 %
W+2 jet	1376	84 $\pm$ 2 %	7.2 $\pm$ 2.2 %	2.2 $\pm$ 0.4 %
W+3 jet	212	81 $\pm$ 4 %	7.5 $\pm$ 2.3 %	2.2 $\pm$ 0.4 %
W+ $\geq$ 4 jet	61	80 $\pm$ 4 %	7.5 $\pm$ 2.3 %	2.2 $\pm$ 0.4 %

Table 9: The various components of the Wc background calculation. The "Real W fraction" accounts for expected contributions from QCD non-W events (measured using the $\not{E}_t$ vs I method described in the text) as well as diboson production and Z events where one lepton has not been reconstructed or where the Z produced a single lepton through the decay Z$\to\tau^+\tau^-$, $\tau \to \ell X$.

missed or where the Z decayed to τ's one of which decayed to a lepton. The expected number of events from these sources is small (less than half of the hadronic non-W contribution calculated with the I vs $\not{E}_t$ method) and has been calculated using Monte Carlo by Guillaume Unal [5]. Table 9 lists the expected real W fraction in the data ($F_{real\ W}$)after accounting for the contribution from these processes.

The fraction of W events with a W$c\bar{s}$ or W$\bar{c}s$ vertex (F_{Wc}) has been calculated using HERWIG Monte Carlo [4]. HERWIG is used since it includes at some level, higher order diagrams like $gg \to Wc\bar{s}$. Because many Wc events are produced from a strange quark from the proton sea, the results are sensitive to the structure functions used in the calculation. A 30 % systematic uncertainty is assigned to the Wc fraction based on studies using a variety of structure functions [8]. The final Wc sample used is generated by HERWIG and uses the MRSD0$'$ parton distribution functions. The predicted Wc fraction (F_{Wc}) as a function of jet multiplicity is shown in Table 9.

The second piece of information needed is the probability of getting a soft lepton tag from the decay of the charm quark ($\epsilon_{SLT\ Wc}$) which can also be derived from the Monte Carlo. Because of low Monte Carlo statistics, the efficiency for soft lepton tagging a Wc event ($\epsilon_{SLT\ Wc}$) is calculated for all W+$\geq$1 jet events and assumed to be constant as a function of jet multiplicity. Note that the Monte Carlo includes the trigger simulation [10] and so should take into account any possible SLT bias due to requiring the presence of a jet over a threshold. The ($\epsilon_{SLT\ Wc}$) values are summarized in Table 9. Putting this all together, the Wc background in the W+jets sample is calculated as

$$N_{Wc\ tags} = N^{[Njet]}_{W\ candidates} \times F_{real\ W} \times F_{Wc} \times \epsilon_{SLT\ Wc}.$$

The results are summarized in Table 10.

10 Z$\to$ $\tau^+\tau^-$ background

Since the Z$\to$ $\tau^+\tau^-$ decay should be straightforward to model, this background is estimated entirely from Monte Carlo. The process of concern is where both tau's decay leptonically, and one is identified as a primary lepton and the other as a (typically high P_t) soft lepton tag. Significant $\not\!\!E_t$ can arise from an imbalance of the four neutrinos produced in the decay, especially when there are additional jets in the event which can arise from initial state radiation. The ISAJET Monte Carlo is used for this calculation. CDF has previously measured the Z production cross-section $\sigma(p\overline{p}\rightarrow ZX \rightarrow e^+e^-X)$= .21 $\pm$ .01 nb [6]. Combining this with the world average $BR(Z \rightarrow e^+e^-)$= 3.366 $\pm$ 0.008 % [2] yields $\sigma(p\overline{p}\rightarrow ZX \rightarrow e^+e^-X)$=6.2 $\pm$ 0.3 nb . The ISAJET Monte Carlo program is used to generate Z$\rightarrow \tau^+\tau^-$ events and and determine the number of predicted tags. The results are normalized to the above cross section and the measured luminosity for the data sample of 90.3 $\pm$ 7.2 pb^{-1}.

To quantify the ability of ISAJET to model the jet multiplicity correctly, the jet multiplicity of the W candidates in data (with F_{non-W} subtracted) is compared to the multiplicity spectrum in a W sample produced by ISAJET. After normalizing to the number of observed W+0 jet events, ISAJET predicts roughly 40 % more events in each jet multiplicity bin than is observed in the data. Based on this study a 50 % systematic uncertainty is assigned to the Z$\rightarrow \tau^+\tau^-$ background estimate. The results are summarized in Table 10.

11 Diboson background

Diboson production (WW or WZ) where a W decays leptonically producing a high P_t lepton with large $\not\!\!E_t$ and the other W or Z decays either to leptons or to heavy flavor pose a potentially serious source of background soft lepton tags in the W sample. There is no published measurement of Diboson production, and so theoretical predictions and Monte Carlo must be used for this background. The latest calculations of the WW, and WZ production cross section [7] predict 9.9 pb, and 2.8 pb respectively. Although the WW cross section is comparable to the theoretical $t\bar{t}$ cross section for M_{top} $\approx$150 GeV, the number of expected events is small after taking into account the appropriate branching fractions. ZZ production is expected to have an even smaller cross section of $\sim$ 1 pb and so is ignored. ISAJET and QFL are used to generate and simulate 10k WW and 28k WZ events. which are normalized to 90.1 $\pm$ 7.2 pb^{-1}, the integrated luminosity for the data sample. As with the Z$\rightarrow \tau^+\tau^-$ background, a 50 % systematic uncertainty is assigned to the ability of ISAJET to model the jet multiplicity spectrum. An additional 30 % uncertainty on the theoretical cross section is added which is approximately the difference between the LO and NLO calculations. Finally there is a 30 % uncertainty due to limited Monte Carlo statistics The final results are summarized in Table 10.

12 Summary of the backgrounds

Table 10 shows good agreement between the background predictions and observed tags in the W+1 and W+2 jet bins and an excess of tags over the expected background in the signal region. The results are displayed graphically in Figure 14.

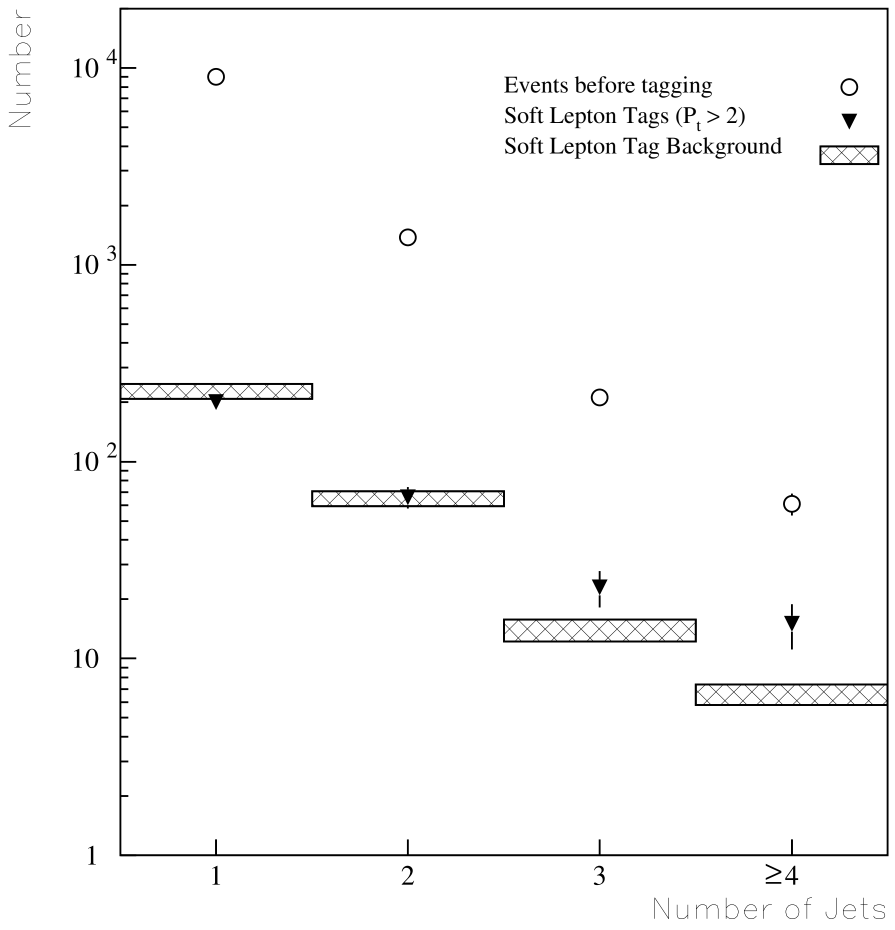

Figure 14: The number of events, observed tags and predicted background tags in the W+jets sample from Run 1b. Boxes show the estimated uncertainty on the background prediction. There is good agreement in the W+1 and W+2 jet bins, and an excess in the W+$\geq$3 jet bins as expected from $t\bar{t}$ production.

BACKGROUND	W+1	W+2	W+3	W+ ≥ 4
(fake+W$b\bar{b}$+W$c\bar{c}$)	202 $\pm$ 18	57 $\pm$ 5	13.2 $\pm$ 1.2	6.1 $\pm$ 0.6
Drell-Yan	-4.9 $\pm$ 3.3	1.6 $\pm$ 2.2	-0.6 $\pm$ 1.4	0.0 $\pm$ 0.6
$b\bar{b}$	16 $\pm$ 8	2 $\pm$ 1	0.4 $\pm$ 0.2	0.12 $\pm$ 0.06
Wc	8.2 $\pm$ 2.3	1.8 $\pm$ 0.5	0.3 $\pm$ 0.1	0.08 $\pm$ 0.02
Z$\rightarrow \tau^+\tau^-$	3.3 $\pm$ 1.4	1.5 $\pm$ 1.1	0.3 $\pm$ 0.1	0.1 $\pm$ 0.05
WW, WZ	3.3 $\pm$ 1.2	1.2 $\pm$ 0.4	0.4 $\pm$ 0.2	0.23 $\pm$ 0.08
TOTAL BACKGROUND	228 $\pm$ 20	65.1 $\pm$ 5.7	14.0 $\pm$ 1.8	6.6 $\pm$ 0.8
OBSERVED TAGS	201	66	23	15

Table 10: Summary of the expected background and observed tags in the W sample. There is good agreement in the W+1 and W+2 jet bins and an excess in the W+$\geq$3 jet bins as expected from $t\bar{t}$ production.

13 Method II Calculation of Run 1b Backgrounds

Since the fake rate from inclusive jets is expected to overestimate the number of tags in the W sample which come from heavy flavor, an alternate method (Method II) is presented here which attempts to calculate explicitly the fake, W$b\bar{b}$ and W$c\bar{c}$ backgrounds. The advantage to this approach is that it in principle does not assume that the heavy flavor content is the same in inclusive jets as in W+jets sample (without top). The disadvantage is that it depends heavily on Monte Carlo and theoretical calculations which carry large uncertainties. It serves, nonetheless, as a more conceptually satisfying check of the background estimate. This is the standard method for the SVX top search in the W+jets channel where the fake background is much lower.

14 The True Fake Rate

First the "fake rate" derived from the inclusive jet sample must be decomposed into two parts - tags which are truly fakes, and tags which originate from heavy flavor decay. This is done by studying the overlap of jets which are b-tagged by the SLT and the SVX. Recall that a *fake* tag is any particle identified as a lepton whose origin is not the a heavy flavor decay. This includes hadrons which pass the lepton selection cuts (such as a pion which fakes an electron or a muon) as well as residual electrons from photon conversions or muons from pions or kaons which decay in flight. A *real* tag in what follows is an e or μ from the semileptonic decay of a b- or c-quark.

Guillaume Unal has applied SVX and soft lepton taggers are applied to a sample of generic jets collected with the JET 50 trigger using Run 1a data [9]. This study should probably be repeated with the higer statistics of Run 1b, but for now we suffer. The conclusions drawn here differ somewhat from those in [9] which calculated the number of SLT tags from b's and not the number of *real* SLT tags from b's which is the number we want here. Guillaume has endorsed the method employed here.

SLT and SVX tags in Jet 50 sample		
SVX tags	1002	
Soft Lepton Tags	453 e	843 μ
In SVX tags:		
SLT's	24 e	33 μ
SLT fake prediction	8.5 e	16.5 μ

Table 11: The number of SVX and soft lepton tags found in a jet sample selected with a JET 50 trigger. The number of soft lepton tags found and predicted by the fake rate are shown for the subset of tracks in SVX tagged jets. A clear excess of soft lepton tags is observed as expected for real heavy flavor events.

The number of SVX tags, as well as the number of soft lepton tags predicted by the SLT fake rate are summarized in Table 11. The sample contains 453 (843) soft electron (muon) tags and 1002 SVX tags. The SVX tagged jets contain 24 (33) soft electron (muon) tags with 8.5 (16.5) predicted by the SLT fake rate. There is a clear excess of SLT's as expected in heavy flavor jets. The SECVTX algorithm also identifies 320 -L_{xy} tagged jets which are expected to be largely mistags originating from mismeasured tracks in non-heavy flavor jets. At the level of accuracy needed for this study, we can assume that these are all mistags and that there are the same number of mistags in the *positive* L_{xy} events. The b purity of SVX tags is then $\sim$ 70 %.

To a good approximation, the number of soft lepton tags from heavy flavor in the sample is given by

$$N_{SLT}^{heavy\ flavor} = \frac{N_{SVX+SLT} - N_{SVX+fake\ SLT}}{\epsilon_{SVX+SLT}}$$

where $N_{SVX+SLT}$ is the number of jets tagged by SLT and SVX, $N_{SVX+fake\ SLT}$ is the number of soft lepton tags in SVX tagged jets predicted by applying the jet-derived fake rate, and $\epsilon_{SVX+SLT}$ is the efficiency for finding a (real) soft lepton tag in a SVX tagged heavy flavor jet. A study of the two taggers in a HERWIG generated jet sample predicts $\epsilon_{SVX+SLT} = 15 \pm 4\%$. Using the numbers from the table and subtracting the expected number of fake SLT tags, this indicates that there are (24-8.5)/0.15 = 103 $\pm$ 44 real electrons and (33-16.5)/0.15=110 $\pm$ 50 real muons in the sample. The uncertainty on these numbers include statistical uncertainties, the systematic uncertainties on the fake rate prediction, and the systematic uncertainty on $\epsilon_{SVX+SLT}$ which covers the ability of the Monte Carlo to model the SVX and SLT. Because this study was not done as a function of P_t or isolation, a further 50% systematic is assigned to the real heavy flavor fraction. Thus 23 $\pm$ 15 % of the electron tags and 13 $\pm$ 9 % of the muon tags in the sample are from real heavy flavor decay. Weighing the two by their relative contributions to the fake rate (see Table 10) and taking into account the correlations of the uncertainties, the jet derived fake rate is determined to contain 16 $\pm$ 10 % real heavy flavor tags, and 84 $\pm$ 10 % fake

Jet Multiplicity	$F_{Wb\bar{b}}$	$F_{Wc\bar{c}}$	$\epsilon_{Wb\bar{b}}$	$\epsilon_{Wc\bar{c}}$
W+ 1 jet	0.6 $\pm$ 0.2 %	1.5 $\pm$ 0.5 %	9 $\pm$ 1 %	3 $\pm$ 1 %
W+ 2 jet	1.1 $\pm$ 0.3 %	3.3 $\pm$ 1.0 %	10 $\pm$ 2 %	3 $\pm$ 1 %
W+ 3 jet	2.2 $\pm$ 0.7 %	6.0 $\pm$ 2.0 %	10 $\pm$ 2 %	5 $\pm$ 1 %
W+ $\geq$ 4 jet	3.6 $\pm$ 1.7 %	6.1 $\pm$ 2.6 %	10 $\pm$ 2 %	5 $\pm$ 1 %

Table 12: The fraction of W+jets events predicted from a HERWIG Monte Carlo simulation of jet events to contain a $b\bar{b}$ or $c\bar{c}$ pair. Systematic uncertainties are estimated by comparing SVX tag rates in a jet sample to HERWIG predictions. Also shown is the soft lepton tag rate for W$b\bar{b}$ and W$c\bar{c}$ events. These numbers are taken from G. Unal's note on the SVX backgrounds [4].

tags. The background due to real fake soft lepton tags is then given by scaling the fake rate prediction by 0.84 $\pm$ .10.

15 W$b\bar{b}$ and W$c\bar{c}$ Backgrounds Using Monte Carlo

The fraction of events in the W+jets sample which are expected to be W$b\bar{b}$ and W$c\bar{c}$ has been estimated for the SVX top analysis using HERWIG and are presented in Table 12 [4]. The uncertainties derive from a comparison of SVX tags in a HERWIG simulation of jet events and jet events in data. The second ingredient needed is the soft lepton tag rate for these events. The results of running the soft lepton tagger on the W$b\bar{b}$ and W$c\bar{c}$ samples are shown in Table 12. There are limited Monte Carlo statistics in the high multiplicity bins, and so the tag rate calculated for W+2 jets is assumed to be valid for the W+3 and W+$\geq$4 jets. The rate does not seem to change from the W+1 to W+2 jet which would tend to support this conclusion. The uncertainties in the table include the systematic uncertainty associated with the Monte Carlo implementation of the SLT algorithm and the statistical uncertainty of the sample. With these inputs, the W$b\bar{b}$ background can be calculated as

$$N_{Wb\bar{b}} = N_{events} \times F_{real\ W} \times F_{Wb\bar{b}} \times \epsilon^{SLT}_{Wb\bar{b}}$$

where the calculation is performed separately for each jet bin and where N_{events} is the number of observed events in the data, $F_{real\ W}$ is the fraction of events in the W sample expected to be real W's (from Table 9), $F_{Wb\bar{b}}$ is the predicted W$b\bar{b}$ fraction and $\epsilon^{SLT}_{Wb\bar{b}}$ is the soft lepton tag efficiency for W$b\bar{b}$. The W$c\bar{c}$ background is calculated in an identical manner.

The results from this method are summarized in Table 13 and compare favorably with those of the standard method. As expected, the standard method yields slightly higher background estimates.

Background	W+1	W+2	W+3	W+$\geq$ 4
fakes	170 $\pm$ 25	48 $\pm$ 7	11 $\pm$ 1.6	5.1 $\pm$ 0.8
W$b\bar{b}$	4 $\pm$ 1.2	1.3 $\pm$ 0.4	0.4 $\pm$ 0.1	0.2 $\pm$ 0.1
W$c\bar{c}$	3.6 $\pm$ 1.1	1.1 $\pm$ 0.3	0.5 $\pm$ 0.2	0.2 $\pm$ 0.1
Other sources	26 $\pm$ 9	8.1 $\pm$ 2.7	0.8 $\pm$ 1.3	0.5 $\pm$ 0.6
Total background	204 $\pm$ 27	59 $\pm$ 8	12.7 $\pm$ 2.1	6.0 $\pm$ 1.0
(Total Background Standard Method)	228 $\pm$ 20	65.1 $\pm$ 5.7	14.0 $\pm$ 1.8	6.6 $\pm$ 0.8

Table 13: Backgrounds calculated using Method II. The fake background is calculated by scaling the fake rate prediction down by 0.84 $\pm$ 0.10 . The W$b\bar{b}$ and W$c\bar{c}$ backgrounds are obtained from HERWIG generated Monte Carlo samples. "Other sources" includes the Z$\rightarrow$ $\tau^+\tau^-$, $b\bar{b}$, Wc, Drell-Yan and Diboson backgrounds which are calculated as in the standard method (Table 10). The background calculated with the standard (fake rate) method is shown for comparison.

16 Properties of SLT Tags in the W Sample

16.1 Stability of the Excess of Tags

If the observed excess of events is truly due to $t\bar{t}$ production it should be robust, and insensitive to small changes in the SLT algorithm. Restricting the analysis to soft electron or muon tags or raising the minimum P_t for SLT tags tests both the reliability of the background estimate in the W+1 and W+2 jet bins and the stability of the excess. Table 14 shows the tags and backgrounds broken down by soft lepton type and for SLT's with P_t > 4 GeV/c. In each case there is an excess of tags in the signal region, and good agreement in the W+1 and W+2 jet bins. A study of HERWIG $t\bar{t}$ events indicates that roughly 3/4 of the excess should come from SLT muon tags, and that 80 % of all tags should have P_t >4 GeV/c. Within the limited statistics available the data is consistent with these predictions.

17 Combined Results from Run 1a and Run 1b Data

For completeness we add the results from the Run 1a data here. These results are for the SLT algorithm including the CMX. The results of the Run 1a and Run 1b analyses, representing 109.4 $\pm$ 7.9 pb^{-1} are presented in Table 15.

References

[1] D. Kestenbaum, Thesis, Harvard University (1996).

	W+1	W+2	W+3	W+ ≥ 4
Soft electrons only				
Total background	53.7 $\pm$ 10	16.7 $\pm$ 3.3	3.9 $\pm$ 1.2	1.6 $\pm$ 0.8
Observed Tags	52	16	7	4
Soft muons only				
Total background	174.6 $\pm$ 17	48.3 $\pm$ 4.6	10.1 $\pm$ 1.4	5.0 $\pm$ 0.6
Observed tags	149	50	16	11
$P_t > 4$ GeV/c				
Total background	101 $\pm$ 13	32.8 $\pm$ 4.2	7.02 $\pm$ 1.4	3.5 $\pm$ 0.6
Observed tags	84	33	15	8

Table 14: The number of observed tags compared to the expectations from background for soft electrons, soft muons and SLT's with the minimum momentum raised to $P_t > 4$ GeV/c in Run 1b. In each case there is good agreement in the W+1 and W+2 jet bins and an excess in the signal region as expected from $t\bar{t}$ production.

	W+1 jet	W+2	W+3	W+$\geq$4
RUN 1A				
Background	W+1	W+2	W+3	W+$\geq$ 4
(fake+W$b\bar{b}$+W$c\bar{c}$)	37.5 $\pm$ 3.8	11.5 $\pm$ 1.1	2.46 $\pm$ 0.25	0.99 $\pm$ 0.1
Drell-Yan	0.35 $\pm$ 0.25	0.10 $\pm$ 0.09	0.05 $\pm$ 0.005	0.05 $\pm$ 0.005
$b\bar{b}$	1.7 $\pm$ 1.2	0.28 $\pm$ 0.2	0.04 $\pm$ 0.02	0.02 $\pm$ 0.01
Wc	3.01 $\pm$ 1.0	0.69 $\pm$ 0.23	0.06 $\pm$ 0.04	0.00 $\pm$ 0.005
Z$\rightarrow \tau^+\tau^-$	.85 $\pm$ .32	.23 $\pm$ 0.10	0.1 $\pm$ 0.03	0.01 $\pm$ 0.005
WW,WZ	0.55 $\pm$ .29	0.20 $\pm$ 0.11	0.16 $\pm$ 0.04	0.02 $\pm$ 0.005
Total background	44.2 $\pm$ 4.1	13.1 $\pm$ 1.2	2.9 $\pm$ 0.3	1.1 $\pm$ 0.1
Observed tags	44	16	4	2
RUN 1A+1B				
Total background	272 $\pm$ 24	78.2 $\pm$ 6.9	16.9 $\pm$ 2.1	7.7 $\pm$ 0.9
Observed tags	245	82	27	17

Table 15: Results of the SLT analysis for Run 1a combined with Run 1b representing 109.4 $\pm$ 7.9 pb^{-1} of data.

[2] Particle Data Group, Phys. Rev. D, **D50** Part I (1994).

[3] S. Kopp, Thesis, The University of Chicago, (1994).

[4] G. Unal, CDF/ANA/TOP/CDFR/3389, (1995).

[5] G. Unal, CDF/ANA/TOP/CDFR/3513, (1995).

[6] F. Abe *et al.* Phys. Rev. D, **68**, 29, (1990).

[7] J. Ohnemus, Phys. Rev. D, **44**, 3477 (1991); J. Ohnemus, Phys. Rev. D, **44**, 1403 (1991).

[8] M. Shaw *et al.*, CDF/ANAL/TOP/CDFR/2252, (1993).

[9] G. Unal *et al.*, CDF/ANAL/TOP/CDFR/2281 (1993).

[10] T. Liss, CDF/DOC/TOP/GROUP/2998 (1995).